University of Arkansas, Fayetteville
ScholarWorks@UARK

Theses and Dissertations

5-2016

Structural Identification of an Elevated Water Tower

James Thomas Norris
University of Arkansas, Fayetteville

Recommended Citation

Structural Identification of an Elevated Water Tower

A thesis submitted in partial fulfillment
of the requirements for the degree of
Master of Science in Civil Engineering

by

James Thomas Norris
Arkansas State University
Bachelor of Science in Civil Engineering, 2011

May 2016
University of Arkansas

This thesis is approved for recommendation to the Graduate Council.

_____
Dr. Ernest Heymsfield
Thesis Director

_____   _____
Dr. W. Micah Hale   Dr. Panneer Selvam
Committee Member   Committee Member

ABSTRACT

Elevated water tanks are generally located at higher elevations within a particular geographic area. The location and height of these structures often makes them desirable for installing wireless and cellular communications antennas. The impact of this practice on the long-term serviceability performance of the primary structure is not clear and could be an important consideration deserving further analysis. This paper presents a case study of an elevated water tank that was motivated by this particular consideration. The structure had been retrofitted with cellular antennas during its service and later experienced fatigue cracking at the fill pipe-tank interface. The owner wished to determine if the addition of the cellular antennas had contributed to this damage. This paper presents a structural identification program that was implemented to determine how wind, water level, and antenna modifications affect the water tank.

ACKNOWLEDGEMENTS

I would like to express my sincere gratitude to my advisor, Dr. Ernest Heymsfiled for his

continuous encouragement and guidance during my study and to my committee members,

Dr. W. Micah Hale and Dr. Panneer Selvam for their enrichment in and outside of the classroom

and for their support during my study.

DEDICATION

This thesis is dedicated to my wife Elizabeth for her unwavering love and encouragement throughout our marriage and my graduate study.

TABLE OF CONTENTS

CHAPTER ONE

INTRODUCTION

1.1 Background

Elevated water tank structures are increasingly being used for mounting cellular providers' antenna arrays since they are tall and are located at high elevations. These antenna arrays are often added after the water tank has been placed in service, and can potentially alter the geometric characteristics and its corresponding structural response due to wind loads. Gabin (2003) and Zienty (2002) state that one of the reasons water tanks are chosen to mount cellular antennas is because restrictive zoning laws sometimes prevent cellular providers from constructing their own tower. Gabin discusses that placing antennas on existing water tanks provides the tank owners with additional revenue through leasing to cellular provider companies but that many problems have occurred from adding them. The specific problems mentioned include structural damage, OSHA violations, and water contamination from improper penetrations into the steel.

The research contained in this study was motivated by a performance problem observed for an elevated water tank structure located in Fayetteville, AR. The water tank is a single pedestal spheroid configuration and was originally constructed in 1975. Cellular antennas were added to the exterior of the structure in 1994, and around 2008, a fatigue crack formed internally where the inlet/outlet pipe connects to the bottom of the tank. The crack was repaired, but the tank owner raised questions as to whether the crack was precipitated by the addition of cellular antennas to the tank, or if it was simply the long-term result of some other issue related to the overall tank design. This particular water tank is very flexible, and lateral displacements can be observed visually. The engineer responsible for retrofitting the tank performed strength design

1

calculations for the additional dead and wind loads imposed on the structure due to the antennas, but serviceability issues such as dynamic displacement and fatigue were not considered in the engineer's calculations and are usually not evaluated for such modifications.

1.2 Objective

In order to evaluate the performance of the water tank, the process of structural identification was utilized. Structural identification is the process of creating and updating a physics-based model of a structure based on its measured responses for use in assessing the health and performance of the structure (Moon et al., 2013). While there are many research examples and case studies focusing on the structural identification of bridges and buildings, there is not much information on the structural identification and performance of elevated water tanks. Even though the process of performing structural identification is similar for different types of structures, elevated water tanks present a unique case in which the mass of the structure changes greatly depending on the water level in the tank; some configurations are very flexible, and the weight of the water in the tank is significantly greater than the self-weight of the tank structure itself.

A review of the available literature related to performance of water tanks suggests that most research is focused on the vibration response of elevated water tanks under seismic loading or the effects of sloshing. One of the earliest examples in the literature showing interest in the vibration response of water tanks was conducted by Carder (1936). Carder studied the vibrations of 37 elevated steel water tanks to better understand their behavior during earthquakes. It appears from Carder's paper that all of the water tanks were multi-column and the water level was always full when they were tested. Moslemi et al. (2011) conducted an analytical study focusing on the fluid interaction for a liquid-filled conical water tank subjected to a specific ground

2

motion. Lopes and Olivera (2012) focused on reducing seismic risk of reinforced concrete water tanks. They studied in-situ ambient data and analytical dynamic properties of 44 water tanks with an ultimate goal of developing an expression that estimates fundamental frequency for multiple water tank configurations. Their research concluded that an expression was developed that can compute the natural frequency for most water tanks.

Experimental studies on the dynamic behavior of water tanks under different wind loads, varying water levels, and tank modifications to support cellular antennas are practically nonexistent in the literature. Consequently, the objective of this research is to determine how wind, water level, and antenna retrofitting affect the dynamic behavior of a single pedestal water tank.

1.3 Scope

There are many load conditions that can affect the behavior of a structure. Two load conditions that affect the dynamic response of a water tank structure include ambient wind and the water level inside the tank. Other load conditions that are beyond the scope of this paper and have the potential to affect the dynamic response of this type of structure include vortex shedding and sloshing. This study focuses on extracting frequencies and displacements from field measured ambient vibration data under various wind speeds and water levels so that the dynamic behavior of the water tank can be revealed.

1.4 Structure Description

The elevated water tank evaluated in this research is a single pedestal spheroid configuration designed by the Chicago Bridge and Iron Company. Figure 1.1 provides views of the water tank exterior, the connection of the inlet/outlet pipe to the tank, and the cellular antennas that were added to the structure. The water tank was built in 1975 and is located in Fayetteville, Arkansas.

3

The height of the water tank is 120 feet. It has a design capacity of 75,000 gallons (Pugh, 1975). The top of the tank is in the form of a sphere with an inside diameter of 27 ft. The sphere tapers down to a cylindrical steel shaft with an inside diameter of 6.5 ft. The shaft flares out near the base and forms a bell shape with a maximum diameter of 16ft. The tank sections are made up of

Figure 1.1. (a) Exterior view of water tank, (b) Cellular antennas attached and (c) Connection of the inlet/outlet pipe to the tank. (Grimmelsman, 2008)

4

A36 steel plates that are welded together. The thickness of the plates varies from 0.392 in. near the bottom of the structure to 0.1875 in. near the top. The water tank is supported on a reinforced concrete ring footing that bears on shale. The available design drawings for the tank indicate that its self-weight is 62.4 kips and maximum design water weight is 630.6 kips.

At the base of the water tank is a door that provides access for maintenance. Once inside the tank, there is a ladder attached to the wall that provides access to the top. The ladder extends up the shaft to the bottom of the tank where a 3 ft. diameter access tube runs through the center of the tank allowing access to the roof. An 8 in. diameter inlet/outlet pipe and a 6 in. diameter overflow pipe are also located inside and run from the ground level up to the tank. The inlet/outlet pipe is insulated and attached to pipe support angle brackets at two different points along the height of the water tank.

CHAPTER 2

EXPERIMENTAL PROGRAM

2.1 Test Description

Ambient vibrations of the water tank were recorded for different operating conditions in order to quantitatively characterize its in-situ behavior by following the structural identification process. Figure 2.1 (b) shows a weather station equipped with an anemometer attached to the top of the water tank that measured wind speed and direction while ambient vibrations were measured. The operating conditions of the tank when ambient vibrations were measured included varying levels of water and wind speeds. Twenty different data sets totaling 52 hours of ambient vibrations were recorded over 17 days during January, 2008. The water level in the tank was controlled by personnel from the city at times during testing. Although the city personnel could control water filling and draining inside the tank, setting the water level for a specific level was unachievable. Consequently, the water levels principally considered for structural identification purposes in this study included the water tank being full and empty. The full water tank case was chosen because water could be heard flowing down the overflow pipe for one data set, indicating the tank was full. The empty water tank case was chosen because draining the tank was relatively simple, and because one data set was recorded when the water tank was completely empty. The additional data sets were collected under various water levels, but the exact level of the water in the tank during testing is uncertain. Ambient vibrations were measured using 12 uniaxial accelerometers that were installed at different elevations along the height of the water tank. The accelerometers used were model 393C accelerometers from Peizotronics, Inc. These accelerometers have a nominal sensitivity of 1 V/g, a frequency range of 0.025 to 800 Hz, and a measurement range of +/- 2.5g. The accelerometers were positioned to measure the ambient vibrations in two

6
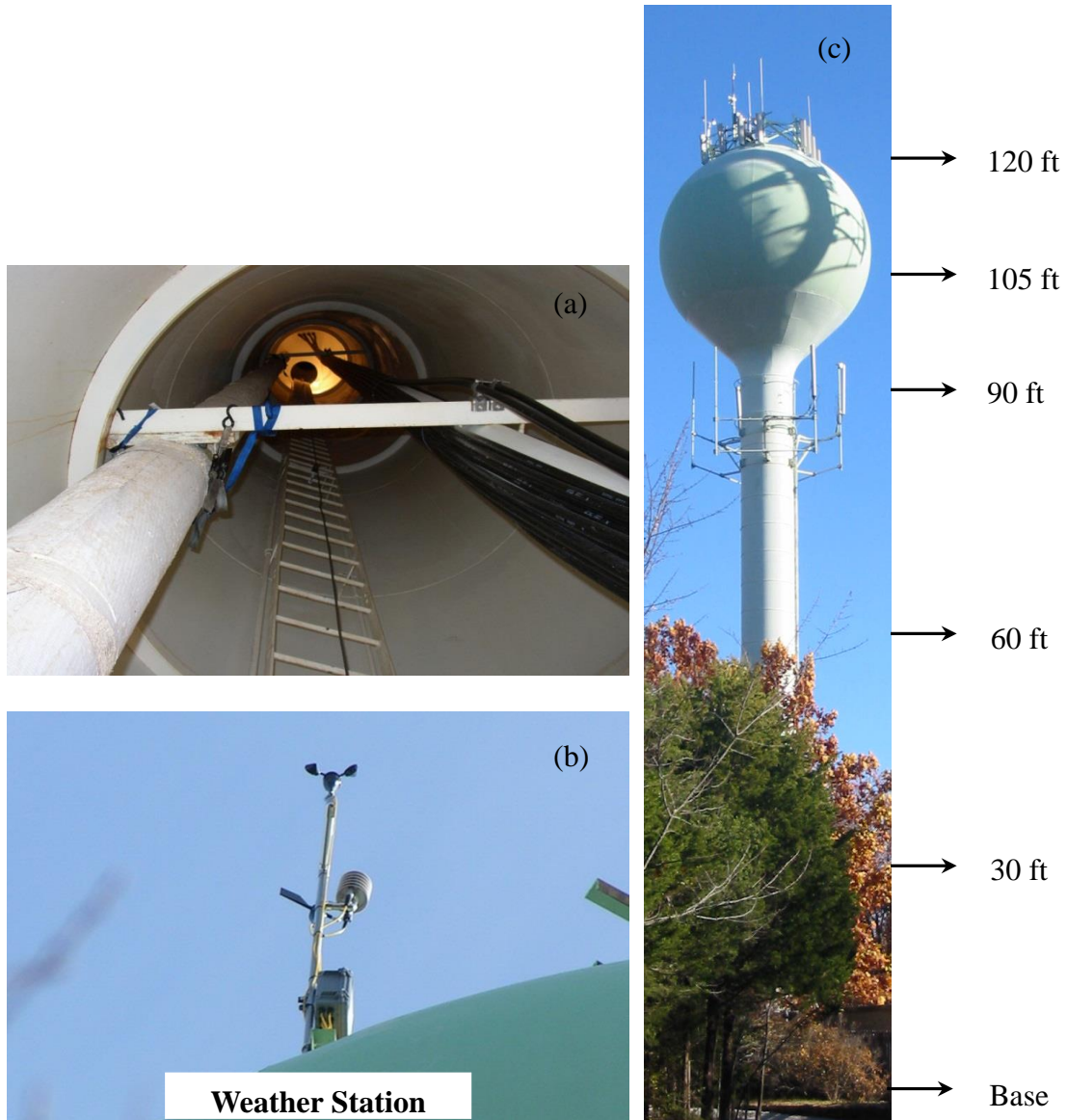
Figure 2.1. (a) Inside view of water tank shaft (b) Weather station and (c) Accelerometer elevations. (Grimmelsman, 2008)

orthogonal directions (x-direction and y-direction). The accelerometers were attached to the

interior of the tank structure using magnets for mounting. Figure 2.1 (c) shows the elevations that

the accelerometers were installed. Coaxial cables were routed from each accelerometer location

to the data acquisition system located at the base. The data acquisition system is manufactured by

National Instruments and is equipped with a PXI mainframe containing Model 4472B dynamic

7

signal acquisition modules. The accelerometers measured continuously at 1 kHz during testing and the data recorded was stored on a hard drive.

CHAPTER 3

DATA ANALYSIS

3.1 Measured Wind Speed Conversion

The weather station has an anemometer located on top of a pole that is mounted to the top of the

water tank, Figure 2.1 (b). The height of the anemometer is approximately 6ft above the tank,

meaning that the wind speeds were measured at approximately 126 feet above ground level,

while the weather station recorded wind speeds at one second intervals. In order to use the

recorded wind speeds for analysis, wind speeds were converted to an equivalent 3-second gust

wind speed measured 33 feet above ground. This represents the standard format for wind speeds

used in ASCE 7-10 (ASCE, 2013). The measured wind speeds were converted to a 3-second gust

wind speed by averaging the measured speed every three seconds and dividing the average by

the appropriate Exposure Coefficient, Kh, for 126 feet above ground level found in ASCE 7-10

(ASCE, 2013). Performing this conversion allows the measured wind speeds to be used to

calculate wind pressures along the height of the structure using the design wind pressure

equations found in ASCE 7-10. The minimum, maximum, and average 3-second gust wind

speeds measured for each data set are shown in Table 3.1.

3.2 Modal Parameter Identification

The ambient vibration measurements were evaluated using two different output-only modal

identification algorithms in order to identify modal parameters of the water tank such as

frequencies and mode shapes. The first algorithm used was stochastic subspace identification

(SSI) algorithm (Van Overschee and De Moor, 1993; Peeters and De Roeck, 1999), which is a

time domain algorithm. The SSI algorithm has been used extensively by many researchers to

identify modal parameters from ambient vibration tests of bridges (Reynders and De Roeck,

9

2008), buildings (Moaveni et al., 2011), and other constructed systems such as towers (Hansen et al., 2006) and chimneys (Brownjohn et al., 2009). The second algorithm used was frequency domain decomposition (FDD). FDD is another output only algorithm and is also widely used in modal identification for various types of structures. FDD is discussed and compared to other modal identification techniques in the research by Moaveni (2011).

Both SSI and FDD were used to identify frequencies and mode shapes from the ambient data. Having two modal identification algorithms identify similar frequencies and mode shapes for a set of data helps reduce uncertainty when identifying modes. Figure 3.1 shows a representative
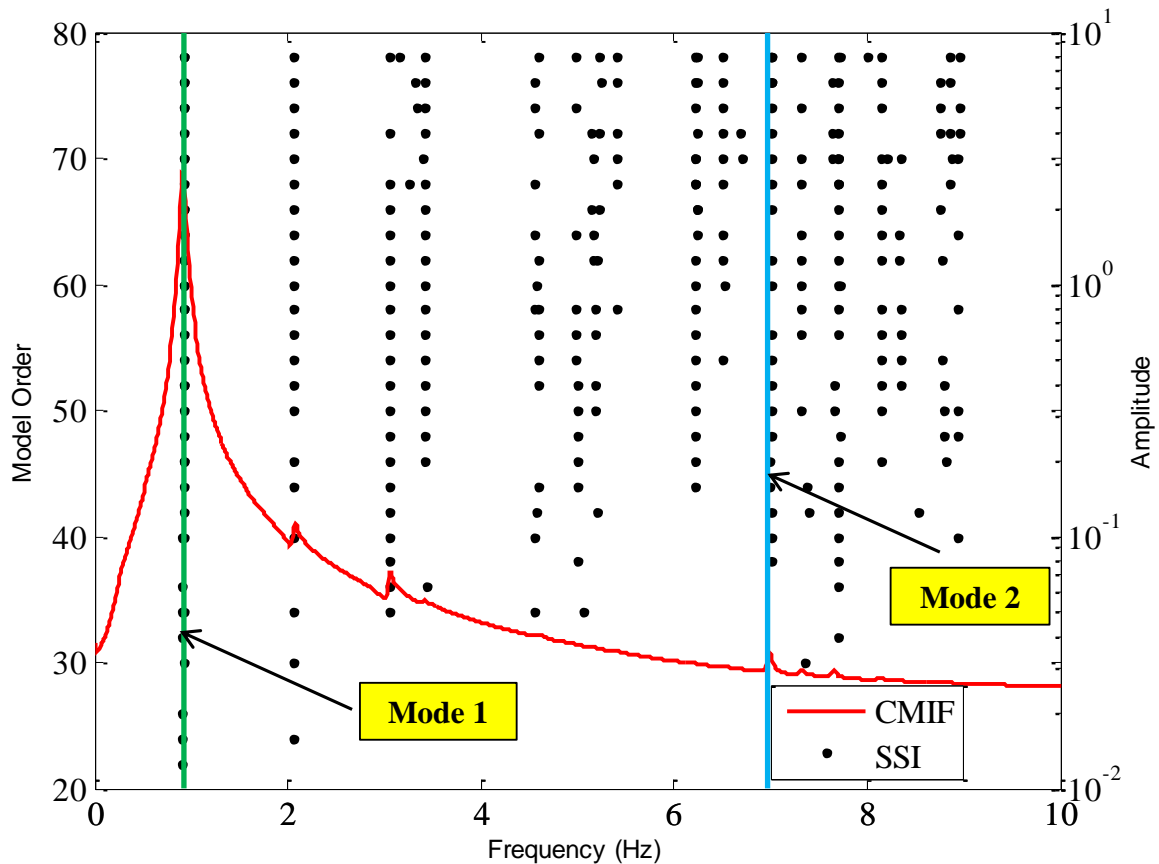

Figure 3.1. Correlation of Stochastic Subspace Identification (SSI) Stability Diagram and Complex Mode Indicator Function (CMIF)

10

plot of a stability diagram with a complex mode indicator function (CMIF) overlaid. The stability diagram is produced from SSI and identifies possible modes for successive orders. Wherever trends are located indicate a stable mode, and the frequency and mode shapes can be extracted to verify the mode is real. The CMIF was generated in the FDD process, and its peaks indicate the frequency where a mode may be present. The SSI stability plot and the CMIF plot are overlaid to show that the modes identified from both algorithms agree with each other.

For a given data set, SSI and FDD were used to extract frequencies and mode shapes. When the frequencies and mode shapes extracted from a data set matched using both FDD and SSI, the mode was determined to be real. Mode 1 was easily captured and had the strongest presence in each data set. This is evident when looking at Figure 3.1. Mode 2 was present in most of the load cases but as seen in Table 3.1, mode 2 was not captured in all of the data sets. Mode 1 was primarily used for structural identification purposes in this paper.

Table 3.1 lists the frequencies identified from each data set for modes 1 and 2 along with the measured 3-second gust wind speeds. The data sets are labeled numerically based on when they were collected in the field. Data sets 9 and 17 represent the known water level data sets for the full tank and the empty tank respectively. The other data sets were collected under various operating conditions but since their exact water level is nonspecific they have been labeled as unknown.

The data in Table 3.1 indicate that the frequencies identified for modes 1 and 2 vary between data sets, with mode 1 showing the largest variation. In order to explain the large variation for mode 1 frequencies, the theoretical equation for the fundamental frequency of a cantilever beam

11

is used. It was chosen because a cantilever beam is a simplified structural model of the water

tank configuration in this research.

TABLE 3.1. Wind Speeds and Frequencies Identified From Ambient Vibrations

Data Set	Water Level During Testing	3-Second Gust Wind Speed During Testing (mph)			Extracted Frequencies From Ambient Vibration Data (Hz)	
		Min	Max	Avg	Mode 1	Mode 2
1	Unknown	2.7	30.0	14.4	0.2737	6.3720
2	Unknown	2.3	32.4	13.9	0.2981	6.3480
3	Unknown	0.9	10.8	5.2	0.3031	6.3480
4	Unknown	2.3	5.1	2.9	0.6073	---
5	Unknown	0.8	10.5	3.6	0.5716	6.860
6	Unknown	2.2	7.7	3.8	0.6172	---
7	Unknown	0.2	12.1	5.0	0.6172	---
8	Unknown	---	---	---	0.4098	6.7140
9	Full	7.9	13.6	10.0	0.2197	6.6890
10	Unknown	3.4	28.8	13.5	0.4639	6.7140
11	Unknown	4.2	25.6	12.9	0.6310	---
12	Unknown	4.5	30.8	14.4	0.6531	6.7090
13	Unknown	2.8	9.8	4.2	0.519	6.86
14	Unknown	2.4	15.5	9.2	0.903	6.812
15	Unknown	1.1	14.2	5.5	0.926	---
16	Unknown	2.3	14.8	7.4	0.9238	---
17	Empty	3.9	16.4	7.9	0.9267	7.007
18	Unknown	3.2	17.6	8.5	0.8447	6.958
19	Unknown	0.9	11.9	4.4	0.9047	6.982
20	Unknown	2.8	24.5	12.6	0.9224	6.958

Note: --- denotes information unavailable

Equation 3.1 shows that the natural frequency of a cantilever beam is a function of its stiffness

and mass. Knowing that the stiffness of a structure is constant, the only remaining variable in

Equation 3.1 that can cause a change in frequency is the mass. A large mass in Equation 3.1

translates to a low frequency, whereas a small mass translates to a high frequency.

$$\omega = \sqrt{\frac{k}{m}} \qquad \text{Equation 3.1}$$

12

Where:

ω = the circular natural frequency (rad/sec)

k = lateral stiffness (lbf/in)

m = the total mass of the system (lbf-sec^2/in)

For this study, the varying water level in the tank represents a change in mass. Consequently, when the water tank is empty, the mode 1 frequency should be higher than for the empty condition. As it fills with water, the frequency should decrease. This behavior is shown in table 3.1.

Data sets 9 and 17 are the two data sets where the water level was known during testing and their mode 1 frequencies indicate that they follow Equation 3.1. Data set 9 was recorded when the tank was full and has the lowest frequency out of all the data sets. Data set 17 was recorded when the tank was empty and has the highest frequency out of all of the data sets. Validating that the data sets 9 and 17 follow Equation 3.1 is important because they will be used in creating and updating a finite element model.

CHAPTER 4

FINITE ELEMENT MODEL DEVELOPMENT

4.1 Finite Element Model Design

A three-dimensional finite element model (FEM) of the water tank was created using the program SAP2000. The main purpose of the FEM in this research is to help characterize the behavior of the water tank by identifying fundamental frequencies due to incremental changes in mass. Knowing the relationship between frequency and mass for varying water levels in the FEM will help identify the water level in the tank for the unknown data sets in Table 3.1.

The water tank was modeled in SAP2000 using 3060 thin shell elements that were designed based on the thickness, diameter, height, and material properties of the steel found in the original water tank design drawings (Pugh, 1975). After the initial FEM was created and before it was revised, it was checked using statics to ensure it was behaving correctly. A simple statics analysis was performed by assigning a vertical load to the top and checking that the sum total of the support reactions generated by the model satisfied force equilibrium.

After the FEM was shown to behave correctly based on the simple statics test, it was revised until it closely matched the modes extracted from data sets 9 and 17. The parameter updating process involved determining the best way to model the water inside the tank, the structure supports, material constants, and shell size so that the mode shapes and frequencies produced by the FEM matched those extracted from data sets 9 and 17. Modeling the water tank according to the steel dimensions and properties obtained from the original design drawings brought the FEM frequencies in close agreement with the identified modes from data sets 9 and 17.

Figure 4.1 shows the first two bending modes generated by the FEM. In order to compare the

mode shapes produced from the FEM to the mode shapes extracted from the ambient
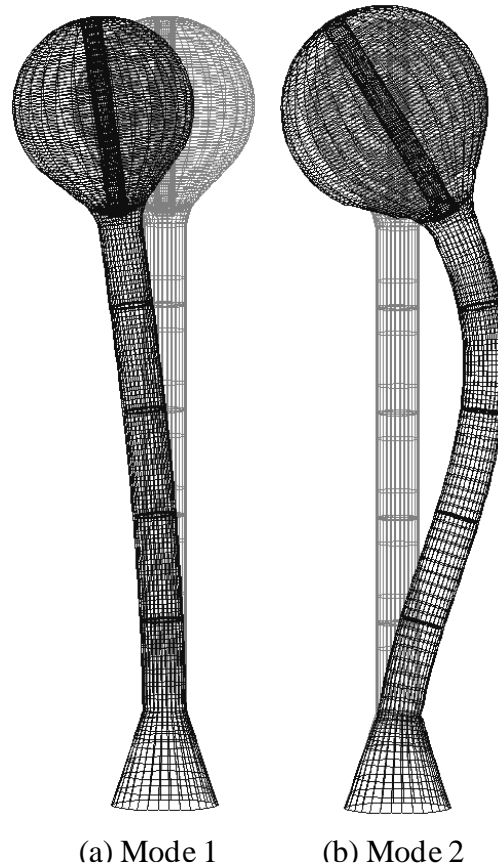

(a) Mode 1   (b) Mode 2

Figure 4.1. Mode 1 and Mode 2 of FEM

data, mode shape values were extracted from the FEM at similar elevations that the

accelerometers were installed at on the water tank. This was done in order to compare mode

shapes from the water tank and from the FEM under similar spatial resolution. Figure 4.2 shows

a comparison of the mode shapes extracted from the ambient data and the mode shapes generated

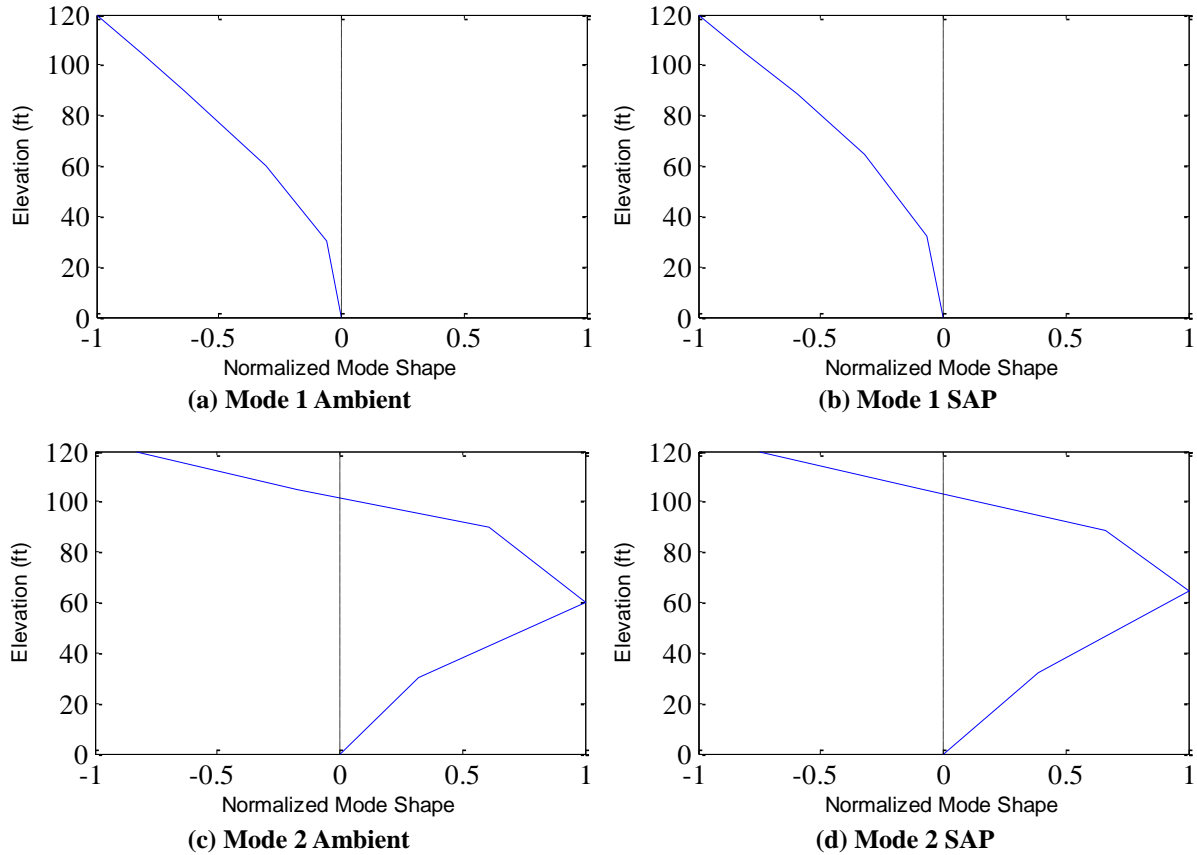by the FEM under similar spatial resolution.

15

Figure 4.2. Ambient and SAP2000 Mode Shapes

Once the FEM was created and updated to match the frequencies extracted from data sets 9 and 17, a dynamic analysis was performed to validate the model frequencies. The dynamic analysis checked the fundamental frequencies generated by the FEM in the context of a single degree of freedom (SDF) system. In order to perform this check the effective lateral stiffness was determined using Equation 4.1. The effective lateral stiffness of the FEM was determined by applying a lateral unit load to a node at the top of the water tank and running the model to generate the corresponding lateral displacement at the node.

$$k = \frac{F}{\Delta}$$
Equation 4.1

Where:

16

www.manaraa.com

F = lateral unit load (kip)

k = effective lateral stiffness (kip/in)

Δ = displacement (in)

The effective lateral stiffness of the FEM was calculated to be 3.49 kip/in. Establishing the

effective lateral stiffness of the FEM, Equation 3.1 can be used to generate fundamental

frequencies for incremental changes in mass. The same incremental mass values can also be

applied as loads to the FEM to produce fundamental frequency results. Table 4.1 shows a

comparison of the fundamental frequencies produced from the FEM and Equation 3.1.

**Table 4.1. Frequency Comparison
of FEM and SDOF Equation 3.1**

Weight (kips)	FEM	SDOF	Percent Difference (%)
36.2	0.984	0.972	1.22
61.4	0.753	0.746	0.93
111.9	0.557	0.553	0.72
137.1	0.503	0.500	0.60
187.5	0.430	0.427	0.70
263.2	0.362	0.361	0.28
364.1	0.308	0.307	0.32
439.8	0.280	0.279	0.36
565.9	0.247	0.246	0.40
666.8	0.227	0.227	0.00

The initial weight starts at 36.2 kips as opposed to zero because in a single degree of freedom

system, the self-weight of the structure is split between its fixed end and free end. A weight of

36.2 kips represents the empty condition of the water tank and is exactly half of the structure

self-weight. The frequency values in Table 4.1 are nearly identical and suggests that the model is

behaving similar to the theoretical equation.

17

The incremental frequency values generated by the FEM in Table 4.1 were plotted against the frequencies of data set 9 and 17 as shown in Figure 4.3. Figure 4.3 indicates that the FEM is calibrated well to the extracted data.
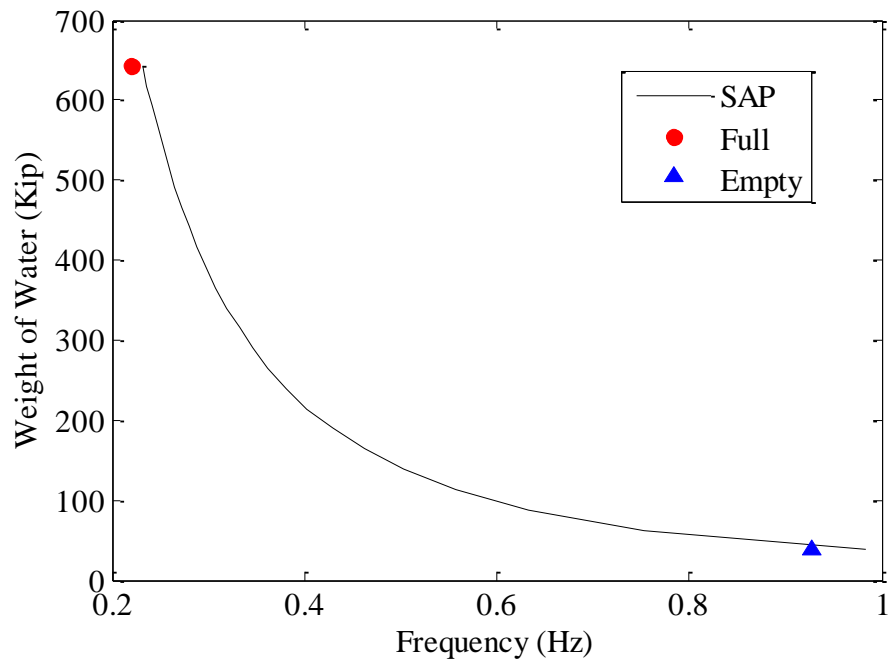

Figure 4.3. Data sets 9, 17, and SAP2000 Frequencies

CHAPTER 5

WATER TANK CHARACTERIZATION

5.1 Reorganized Data Sets

The frequency curve generated by the FEM shown in Figure 4.3 reveals the relationship between the weight of the water in the tank and its corresponding modal frequency. Having this curve is beneficial because the water level for the unknown data sets in Table 3.1 can be estimated based on their extracted frequency. Table 5.1 shows the data sets from Table 3.1 rearranged based on the percentage of water in the tank. The weight of water in the tank was estimated by comparing

Table 5.1. Data Sets Reorganized by Percentage of Tank Capacity

Data Set	Percentage of tank capacity (%)	Before (Table 3.1)	After	Extracted Frequencies from Ambient Vibration Data	
				Mode 1	Mode 2
17	5.6	Empty	Empty	0.9267	7.007
15	5.6	Unknown	Empty	0.926	---
16	5.7	Unknown	Empty	0.9238	---
20	5.7	Unknown	Empty	0.9224	6.958
19	5.9	Unknown	Empty	0.9047	6.982
14	5.9	Unknown	Empty	0.903	6.812
18	6.8	Unknown	Empty	0.8447	6.958
12	11.3	Unknown	Slightly Full	0.6531	6.709
11	12.1	Unknown	Slightly Full	0.631	---
6	12.7	Unknown	Slightly Full	0.6172	---
7	12.7	Unknown	Slightly Full	0.6172	---
4	13.1	Unknown	Slightly Full	0.6073	---
5	14.8	Unknown	Slightly Full	0.5716	6.86
13	17.9	Unknown	Moderately Full	0.519	6.86
10	22.4	Unknown	Moderately Full	0.4639	6.714
8	28.7	Unknown	Moderately Full	0.4098	6.714
3	52.5	Unknown	half full	0.3031	6.348
2	54.3	Unknown	half full	0.2981	6.348
1	64.4	Unknown	half full	0.2737	6.372
9	100.0	Full	Full	0.2197	6.689

the identified frequencies in Table 3.1 to the curve shown in Figure 4.3. The data sets were then rearranged based on a percentage of water in the tank associated with their identified frequencies. Establishing the water level for the remaining data sets is a result of the structural identification process. Field measured data is often gathered under less than ideal conditions where not all parameters are known. Having an FEM updated based on a couple of known sets of data has provided a way for the water level to be estimated for the remaining data sets.

5.2 Water Tower Displacements

The acceleration data was converted to displacement in order to further characterize the behavior of the water tank. The method for converting acceleration measurements into displacement is discussed in Slifka (2004). Slifka explains the issues of DC bias associated with accelerometers and the lack of initial conditions that can lead to significant errors when performing integration. Slifka shows how filtering the data throughout the integration process can minimize these errors. The basic procedure for converting acceleration to displacement is shown in Figure 8.

| Filter | ➡ | Integrate | ➡ | Filter | ➡ | Integrate | ➡ | Filter |

Figure 8. Filter and Integration Flow Chart

The process shown in Figure 8 was coded and executed in MATLAB. The trapezoidal rule and a Butterworth filter were chosen for integration and filtering the data respectfully. Frequency cutoffs of 0.1 Hz and 24 Hz were used in the filtering process. Most of the frequencies captured in the data were between these two frequencies which is why they were chosen. The first integration converts acceleration to velocity and the second integration converts velocity to displacement. Time history plots of displacement were generated for all of the data sets in Table

20

5.1. Data sets 9, 2, and 17 were chosen as the representative displacement plots for the tank full, half full, and empty conditions respectively. The relationship between the displacement of the water tank and the water level in the tank is shown in Figure 5.1. The displacements shown in Figure 5.1 indicate displacement magnitude varies depending on the water level.
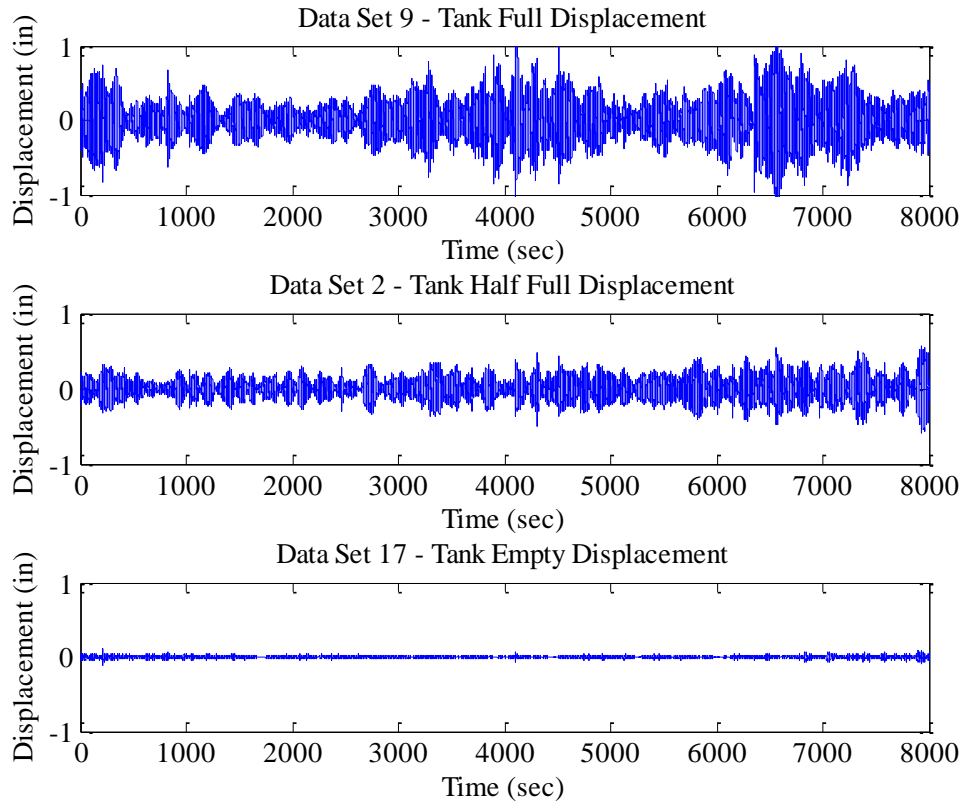

Figure 5.1. Time History Displacement for Tank Full, Half Full, and Empty

In order to see if there is a correlation between the water tank's displacement and the recorded wind speeds, Figure 5.2 was created. Figure 5.2 was created by plotting the water tank's displacement and associated wind speed at the time the displacement occurred. Figure 5.2 shows that the displacements under the lower recorded wind speeds are similar to the displacements at higher recorded wind speeds. To help explain why the displacements are similar over the range

www.manaraa.com

of recorded wind speeds, Figure 5.3 was created. Figure 5.3 shows the relationship between the basic 3-second gust wind speed and velocity pressure, using the velocity pressure equation found in ASCE 7-10 (ASCE, 2013). A simplified velocity pressure equation is used without any of its typical coefficients. Looking at the equation shown in Figure 5.3, one can see that the velocity pressure is a function
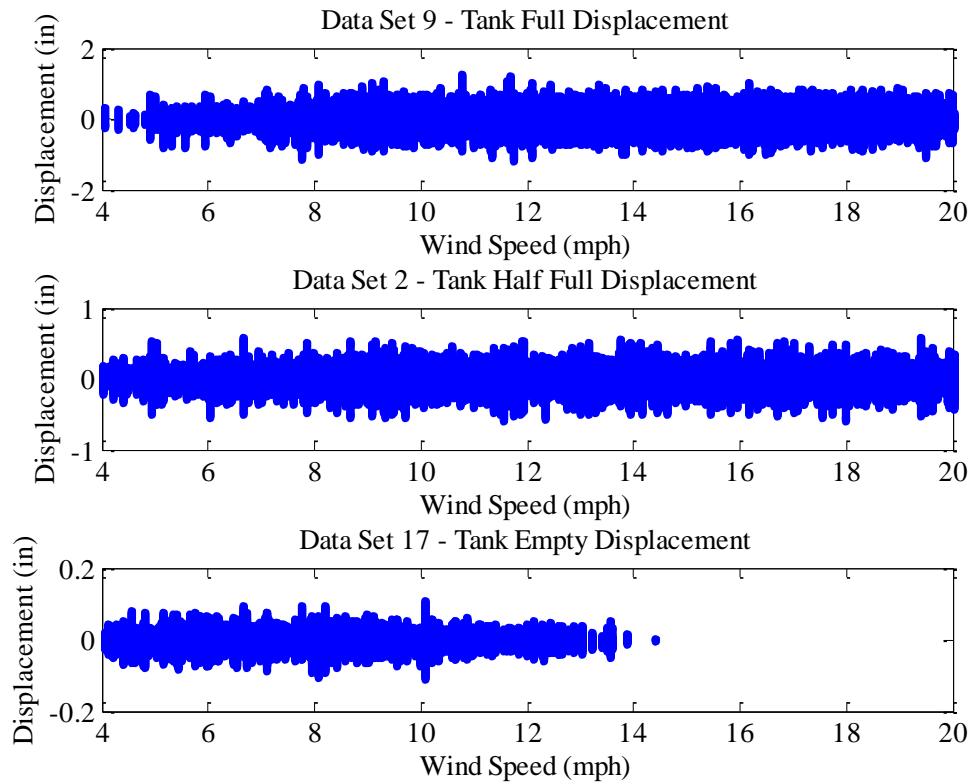

Figure 5.2. Wind Speed Displacement for Tank Full, Half Full, and Empty

of the air density coefficient multiplied by the velocity squared. Looking back at Table 3.1, it shows that the largest measured 3-second gust wind speed is 32.4 mph, which occurred in data set 2. All other measured wind speeds fall under 32.4 mph. This means the velocity pressure acting on the water tank during each data set falls on the lower bound of the curve in Figure 5.3.

This indicates that the velocity pressure did not vary significantly with respect to the measured wind speeds and is most likely the reason why Figure 5.2 does not show a trend between displacement and wind speed.
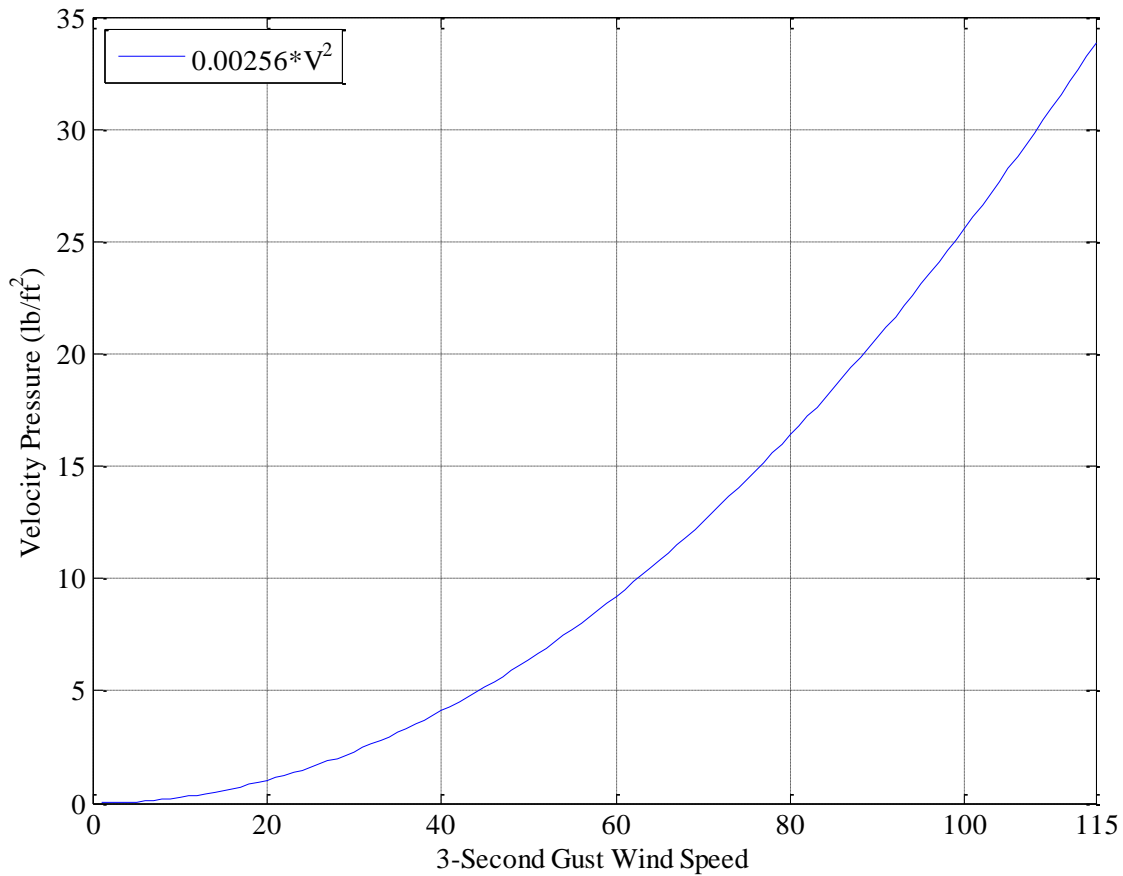

Figure 5.3. Change in Velocity Pressure With Respect to Wind Speed

5.3 P-Delta Effects

The weight of the water inside the tank can be significantly heavier than the self-weight of the structure. The relationship shown in Figure 5.1 suggests that the water level inside the tank influences the water tank's displacement. In order to determine if the water level inside the tank is causing second-order displacements and to explain the trend shown in Figure 5.1, P-Delta

23

effects were investigated. Equations 5.1 through 5.4 were used to investigate P-Delta effects on the water tank.

$$\Delta = \frac{F}{k} \qquad\qquad \text{Equation 5.1}$$

$$M_1 = F_1(L) + P(\Delta_1) \qquad\qquad \text{Equation 5.2}$$

$$F = \frac{M}{L} \qquad\qquad \text{Equation 5.3}$$

$$M_n = M_1 + P(\Delta_2 - \Delta_1) \dots + P(\Delta_{n+1} - \Delta_n) \qquad\qquad \text{Equation 5.4}$$

Where:

F = lateral load (kip)

k = effective lateral stiffness (kip/in)

$\Delta_{1,2,..n}$ = displacement for a given iteration (in)

$M_{1,2,..n}$ = moment at base of tank for a given iteration (kip-in)

P = weight of water in tank (kip)

L = height of lateral load (in)

Equation 4.1 was re-written in terms of displacement and is expressed in Equation 5.1. Equation 5.1 shows that the displacement of a cantilever water tank is a function of its stiffness and a lateral load. Calculating the initial displacement using Equation 5.1, Equation 5.2 can be used to determine the moment from the initial lateral load plus the weight of water multiplied by displacement. Equation 5.3 is used to calculate a new lateral load, and the new lateral load is

24

substituted back into Equation 5.1 to calculate the increased displacement due to the weight of the water. The added displacement is subtracted from the previous iteration and plugged into Equation 5.4. This process continues until the calculated displacement converges.

The lateral load in Equation 5.2 is an idealized representation of the wind load that occurs in the field. In actuality, the water tank is acted upon by a varying wind load that increases along the height of the water tank. For simplicity, the P-Delta effects of the water tank are investigated using a unit lateral load. Using a unit lateral load simplifies the results by limiting the change in displacement due to the water level inside the tank. The P-Delta effects due to an idealized unit wind load are presented in Table 5.2.

Table 5.2 shows that the "tank empty" scenario sees a zero percent change in displacement due to no second order P-Delta effects. The percent change in displacement for the half full and full

Table 5.2. Displacement Amplification

F (kip) =	1.00	**L (in) =**	1242.00	**k (kip/in)=**		3.49
	Tank Empty		**Tank Half Full**		**Tank Full**	
Iteration (#)	**P (kip) =**	0.00	**P (kip) =**	315.30	**P (kip) =**	630.60
	Delta (in)	**M (k-in)**	**Delta (in)**	**M (k-in)**	**Delta (in)**	**M (k-in)**
0.00	0.2865	1242.00	0.2865	1332.34	0.2865	1422.69
1.00	0.2865	1242.00	0.3074	1338.92	0.3282	1448.97
2.00	0.2865	1242.00	0.3089	1339.39	0.3343	1452.80
3.00	0.2865	1242.00	0.3090	1339.43	0.3352	1453.35
4.00	0.2865	1242.00	0.3090	1339.43	0.3353	1453.44
5.00	0.2865	1242.00	0.3090	1339.43	0.3353	1453.45
% Change in Displacement	0.00		7.84		17.02	

scenarios show that the displacement of the water tank is amplified by the weight of water inside the tank. Table 5.2 reveals that for any given lateral load, the half full and full cases will amplify displacements by 7.84 and 17.02 percent respectfully. The results in Table 5.2 suggest that the trend observed in Figure 5.1 is the result of second order P-Delta effects due to the weight of the water inside the tank. This means that the displacement amplification of the structure is a result of its own service loads and would have been present before the antennas were installed.

CHAPTER 6

CONCLUSIONS

A performance problem in the form of a crack prompted this study of structural identification to characterize the water tank's behavior and investigate possible causes of the fatigue crack. Analyzing the water tank's displacement revealed that the wind speeds recorded in the field during this study do not correlate with the variation in displacements observed for the full, half full, and empty data sets: however the variation in displacement does show a strong correlation with the amount of water inside the tank. The investigation of P-Delta effects revealed that the water level inside the tank magnifies the initial displacements due to wind and is the source of the variation in displacement observed for the full, half full, and empty data sets.

Observing that the water level inside the tank influences its displacement is important because it shows that the antennas are not the only source affecting the water tank's displacement. The effect that the antennas have on the water tank's displacement is best represented by the water tank empty data set. A water tank empty condition represents the scenario where the only influence on the water tank's displacement is from wind acting on the tank and the antennas. The data shows that the water tank experienced the least amount of displacement when the water tank was empty. As the water level increases to a full condition, the displacement is observed to be significantly greater than the empty data set. This indicates that the water level inside the tank has a greater influence on its displacement than the antennas under the wind speeds recorded in the field.

27

REFERENCES

ASCE. (2013). *Minimum design loads for buildings and other structures* American Society of Civil Engineers. doi:doi:10.1061/9780784412916

Brownjohn, J. M. W., Carden, P., Goddard, C., & Oudin, G. (2009). Real-time performance monitoring of a TMD for a 183m reinforced concrete chimney. 4th International Conference on Structural Health Monitoring of Intelligent Infrastructure, SHMII 2009, July 22, 2009 - July 24

Carder, D. S. (1936). Observed vibrations of steel water towers. Bulletin of the Seismological Society of America.

Gabin, I. (2003). Installing wireless antennas on water tanks - remember, it's our tank, not their tower. Journal / American Water Works Association, 95(2), 43-44.

Grimmelsman, K. (2008, January 15). *Fayetteville Water Tower Photos* [Photograph]. Fayetteville.

Hansen, M. H., Thomsen, K., Fuglsang, P., & Knudsen, T. (2006). Two methods for estimating aeroelastic damping of operational wind turbine modes from experiments. *Wind Energy, 9*(1-2), 179-191. doi:10.1002/we.187

Lopes, H. M., & Oliveira, C. S. (2012). Use of in-situ dynamic measurements to calibrate analytical models of RC-elevated water tanks. *Shock and Vibration, 19*(5), 903-914. doi:10.3233/SAV-2012-0698

Moaveni, B., He, X., Conte, J. P., Restrepo, J. I., & Panagiotou, M. (2011). System identification study of a 7-story full-scale building slice tested on the UCSD-NEES shake table. *Journal of Structural Engineering, 137*(6), 705-717. doi:10.1061/(ASCE)ST.1943-541X.0000300

Moon, F., & Catbas, N. (2013). Structural identification of constructed systems. (pp. 1-17) American Society of Civil Engineers. doi:doi:10.1061/9780784411971.ch01

Moslemi, M., Kianoush, M. R., & Pogorzelski, W. (2011). Seismic response of liquid-filled elevated tanks. *Engineering Structures, 33*(6), 2074-2084. doi:10.1016/j.engstruct.2011.02.048

Peeters, B., & De Roeck, G. (1999). Reference-based stochastic subspace identification for output-only modal analysis. *Mechanical Systems and Signal Processing, 13*(6), 855-878. doi:10.1006/mssp.1999.1249

Pugh, Robert, comp. *75 MG Watersphere City of Fayetteville, Arkansas*. 29 Jan. 1975. Structural Design Drawings by Chicago Bridge & Iron Company.

Reynders, E., & Roeck, G. D. (2008). Reference-based combined deterministic-stochastic subspace identification for experimental and operational modal analysis. *Mechanical Systems and Signal Processing, 22*(3), 617-637. doi:10.1016/j.ymssp.2007.09.004

Slifka, L. D. (2004). An accelerometer based approach to measuring displacement of a vehicle body. *Master of Science in Engineering, Department of Electrical and Computer Engineering, University of Michigan–Dearborn*

Van Overschee, P., & De Moor, B. (1993). Subspace algorithms for the stochastic identification problem. *Automatica, 29*(3), 649-660. doi:10.1016/0005-1098(93)90061-W

Zienty, D. (2002). Tanks pull double duty. *Water Engineering and Management, 149*(2), 9-13.